MULTIVARIATE TENSOR-BASED MORPHOMETRY ON SURFACES: APPLICATION TO MAPPING VENTRICULAR CHANGES IN HIV/AIDS

Yalin Wang[1,2]*, Jie Zhang* [3]*, Tony F. Chan*[1]*, Arthur W. Toga*[2]*, Paul M. Thompson*[2]

[1] Mathematics Department, UCLA
[2] Lab. of Neuro Imaging and Brain Research Institute, UCLA School of Medicine
[3] Statistics Department, University of Wisconsin-Madison
{ylwang,chan}@math.ucla.edu, jiezhang@stat.wisc.edu, {arthur.toga, thompson}@loni.ucla.edu

ABSTRACT

We apply multivariate tensor-based morphometry to study lateral ventricular surface abnormalities associated with HIV/AIDS. We use holomorphic one-forms to obtain a conformal parameterization of ventricular geometry, and to register lateral ventricular surfaces across subjects. In a new development, we computed new statistics on the Riemannian surface metric tensors that encode the full information in the deformation tensor fields. We applied this framework to 3D brain MRI data, to map the profile of lateral ventricular surface abnormalities in HIV/AIDS (11 subjects). Experimental results demonstrated that our method powerfully detected brain surface abnormalities. Multivariate Hotelling's T^2 statistics on the local Riemannian metric tensors, computed in a log-Euclidean framework, detected group differences with greater power than other surface-based statistics including the Jacobian determinant, largest and least eigenvalue, or the pair of eigenvalues of the Jacobian matrix. Computational anatomy studies may therefore benefit from surface parameterization using differential forms and tensor-based morphometry, in the log-Euclidean domain, on the resulting surface tensors.

Index Terms— Multivariate Tensor-Based Morphometry, Holomorphic One-Form, Surface Modeling

1. INTRODUCTION

Deformation-based morphometry (DBM) [1, 2, 3, 4] uses deformations obtained from the nonlinear registration of brain images to infer local differences in brain volume or shape. Tensor-based morphometry (TBM) [5, 6, 7] tends to examine high-order spatial derivatives of the deformation maps registering brains to common template, constructing morphological tensor maps such as the Jacobian determinant, torsion or vorticity. One advantage of TBM is that it derives local derivatives and tensors from the deformation for further analysis, and statistical maps can be made to localize regions with significant group differences or changes over time. In this paper, we pursue the notion that TBM can even be applied to surface models, making use of the Riemannian surface metric to characterize local surface changes.

The lateral ventricles - fluid-filled structures deep in the brain - are often enlarged in disease and can provide sensitive measures of disease progression [8, 9, 10, 11]. Ventricular changes reflect atrophy in surrounding structures, and ventricular measures and surface-based maps can provide sensitive assessments of tissue reduction that correlate with cognitive deterioration in illnesses.

In this paper, we propose a new multivariate TBM framework for surface morphometry, using differential forms as the basis for the tensors that are analyzed. In an empirical study of brain abnormalities in HIV/AIDS, we studied lateral ventricular surface deformation. We found that the proposed multivariate TBM detected areas of statistically significant deformation even in a relatively small test dataset - from 11 subjects with HIV/AIDS and 8 matched healthy controls. For comparison, we also applied other four TBM statistics to the same dataset. The proposed multivariate TBM proved to have more detection power by detecting consistent but more statistically significant areas of surface deformation. This works complements ongoing work by others, extracting models of ventricular surfaces via fluid registration, and detecting group differences using either M-reps or support vector machines [9, 10, 11].

2. SURFACE CONFORMAL PARAMETERIZATION WITH HOLOMORPHIC ONE FORMS

To register lateral ventricular surfaces across subjects, we applied a canonical conformal parameterization method. Holomorphic one-forms, a structure used in differential geometry, can be used to generate canonical conformal parametrization on a set of simply connected 3D surfaces [12], maximizing

This work was funded by the National Institutes of Health through the NIH Roadmap for Medical Research, Grant U54 RR021813 entitled Center for Computational Biology (CCB). The work was performed while the third author was on leave at the National Science Foundation as Assistant Director of the Directorate for Mathematics & Physical Sciences.

the uniformity of the induced grid over the entire domain.

A summary of canonical conformal parametrization now follows, abbreviated due to the page limit, (see [12] for a more detailed algorithm description).

(1). Compute exact harmonic one-forms basis;

(2). Compute closed harmonic one-forms basis;

(3). Compute holomorphic one-forms basis;

(4). Compute the canonical holomorphic one-form and the canonical conformal parameterization.

Even though the ventricular geometry consists of several branches that are not readily parameterized using other methods, the holomorphic one-forms can be used to induce a smooth conformal grid on the long and narrow horned surfaces of the lateral ventricles, with a differentiable parameterization at the surface junctions. Even though ventricular shape varies widely in normal populations, the curved junctions between the horns are consistently recovered using the differential form method, allowing us to segment the ventricular surface consistently and match each of them via their conformal coordinates.

3. MULTIVARIATE TENSOR-BASED MORPHOMETRY

3.1. Derivative Map

Suppose $\phi : S_1 \rightarrow S_2$ is a map from the surface S_1 to the surface S_2. For simplicity, we use the isothermal coordinates of both surfaces for the arguments. Let $(u_1, v_1), (u_2, v_2)$ be the isothermal coordinates of S_1 and S_2 respectively. The Riemannian metric of S_i can be represented as $\mathbf{g}_i = e^{2\lambda_i}(du_i^2 + dv_i^2), i = 1, 2$.

In the local parameters, the map ϕ can be represented as $\phi(u_1, v_1) = (\phi_1(u_1, v_1), \phi_2(u_1, v_1))$. The *derivative map* of ϕ is the linear map between the tangent spaces, $d\phi : TM(p) \rightarrow TM(\phi(p))$, induced by the map ϕ. In the local parameter domain, the derivative map is the Jacobian of ϕ,

$$d\phi = \begin{pmatrix} \frac{\partial \phi_1}{\partial u_1} & \frac{\partial \phi_1}{\partial v_1} \\ \frac{\partial \phi_2}{\partial u_1} & \frac{\partial \phi_2}{\partial v_1} \end{pmatrix}.$$

Let the position vector of points on S_1 be $\mathbf{r}(u_1, v_1)$. Denote the tangent vector fields as $\frac{\partial}{\partial u_1} = \frac{\partial \mathbf{r}}{\partial u_1}, \frac{\partial}{\partial v_1} = \frac{\partial \mathbf{r}}{\partial v_1}$. Because (u_1, v_1) are isothermal coordinates, $\frac{\partial}{\partial u_1}$ and $\frac{\partial}{\partial v_1}$ only differ by a rotation of $\pi/2$. Therefore, we can construct an orthonormal frame on the tangent plane on S_1 as $\{e^{-\lambda_1}\frac{\partial}{\partial u_1}, e^{-\lambda_1}\frac{\partial}{\partial v_1}\}$. Similarly, we can construct an orthonormal frame on S_2 as $\{e^{-\lambda_2}\frac{\partial}{\partial u_2}, e^{-\lambda_2}\frac{\partial}{\partial v_2}\}$.

The derivative map under the orthonormal frames is represented by:

$$d\phi = e^{\lambda_2 - \lambda_1} \begin{pmatrix} \frac{\partial \phi_1}{\partial u_1} & \frac{\partial \phi_1}{\partial v_1} \\ \frac{\partial \phi_2}{\partial u_1} & \frac{\partial \phi_2}{\partial v_1} \end{pmatrix}.$$

In practice, smooth surfaces are approximated by triangle meshes. The map ϕ is approximated by a simplicial map, which maps vertices to vertices, edges to edges and faces to faces. The derivative map $d\phi$ is approximated by the linear map from one face $[v_1, v_2, v_3]$ to another one $[w_1, w_2, w_3]$. First, we isometrically embed the triangle $[v_1, v_2, v_3]$,$[w_1, w_2, w_3]$ onto the plane $\mathbb{R}^2$; the planar coordinates of the vertices of v_i, w_j are denoted using the same symbols v_i, w_j. Then we explicitly compute the linear matrix for the derivative map $d\phi$,

$$d\phi = [w_3 - w_1, w_2 - w_1][v_3 - v_1, v_2 - v_1]^{-1}. \quad (1)$$

3.2. Multivariate Tensor-Based Statistics

In our work, we use multivariate statistics on deformation tensors [13] and adapt the concept to surface tensors. Let J be the derivative map and define the deformation tensors as $S = (J^T J)^{1/2}$. Instead of analyzing shape differences based on the eigenvalues of the deformation tensor, we consider a new family of metrics, the "Log-Euclidean metrics" [14]. These metrics make computations on tensors easier to perform. Tensors are first transformed via a logarithmic transformation to form a vector space, and statistical parameters may then be computed easily using standard formulae for Euclidean spaces [15].

We apply Hotelling's T^2 test on sets of values in the log-Euclidean space of the deformation tensors. We stack the log-transformed tensor components into a vector, and given two groups of n-dimensional vectors S_i, $i = 1, ..., p$, T_j, $j = 1, ..., q$, we use the Mahalanobis distance M to measure the group mean difference,

$$M = (log\bar{S} - log\bar{T})\Sigma^{-1}(log\bar{S} - log\bar{T})$$

where $\bar{S}$ and $\bar{T}$ are the means of the two groups and Σ is the combined covariance matrix of the two groups.

4. EXPERIMENTAL RESULTS

4.1. Automatic Lateral Ventricular Surface Registration via Holomorphic One-Forms

The concave shape, complex branching topology and narrowness of the inferior and posterior horns have made it difficult for surface parametrization approaches to impose a grid on the entire structure without introducing significant area distortion. To model the lateral ventricular surface, we automatically locate and introduce three cuts on each ventricle. The cuts are motivated by examining the topology of the lateral ventricles, in which several horns are joined together at the ventricular "atrium" or "trigone". We call this topological model, creating a set of connected surfaces, a *topology optimization* operation. After modeling the topology in this way, a lateral ventricular surface, in each hemisphere, becomes an open boundary surface with 3 boundaries(Fig. 1(a)). We computed the exact harmonic one-form

(Fig. 1(b)), its conjugate one-form (Fig. 1(c)), canonical holomorphic one-form (Fig. 1(d)). With the induced conformal net (Fig. 1(e)), each lateral ventricular surface can be divided into 3 connected pieces (Fig. 1(f)). Although surface geometry is widely variable across subjects, the zero point locations of these differential forms are intrinsically determined by the surface conformal structures, and the partitioning of the surface into component meshes is highly consistent across subjects. Figure 1(f) illustrates the automatic surface segmentation results for the same pair of lateral ventricular surfaces, which is similar to the manual surface segmentation results used in prior research [8]; even so it improves on past work as it avoids arbitrarily chopping the surface into 3 parts using a fixed coronal plane.

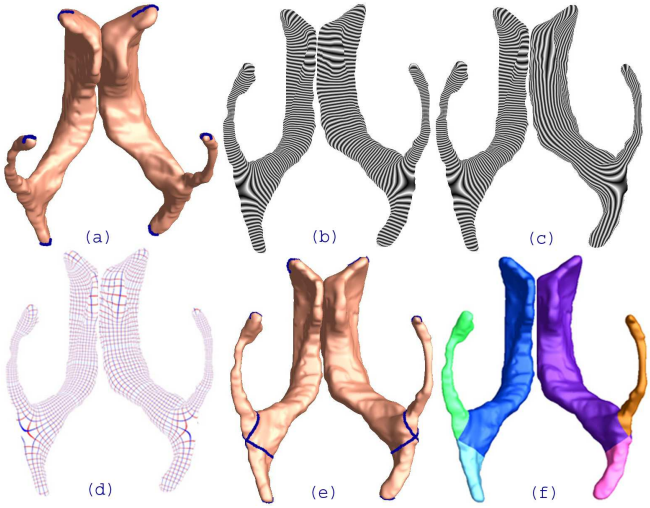

Fig. 1. Automatic lateral ventricular surface partitioning and parameterization using holomorphic one-forms.

After surface segmentation, each lateral ventricular surface is divided to three surfaces, each topologically equivalent to a cylinder. For each piece, we applied holomorphic flow segmentation algorithm again on it and conformally mapped it to a rectangle. Then we register the surfaces across subjects by pairing up corresponding coordinates in the parameter domain [12]. Figure 2 shows an example of a left lateral ventricular surface. After segmentation, each of its three segments is conformally mapped to a rectangle. The computed canonical holomorphic one-form and parameterization results are also shown.

4.2. Multivariate Tensor-Based Morphometry Study on Lateral Ventricular Surface of HIV/AIDS

In our experiments, we compared ventricular surface models extracted from 3D brain MRI scans of 11 HIV/AIDS individuals and 8 control subjects [8]. After surface registration, we computed the surface Jacobian matrix and applied multivariate tensor-based statistics to study differences in ventricular surface morphometry. We ran a permutation test with 5000 random assignments of subjects to groups to estimate the statistical significance of the areas with group differences in surface morphometry. We also used a statistical threshold of $p = 0.05$ at each surface point to estimate the overall significance of the experimental results by non-parametric permutation test [16]. The experimental results are shown in Figure 3(a). After fixing the template parametrization, we used Log-Euclidean metrics to establish a metric on the surface deformation tensors at each point, and conducted a permutation test on the suprathreshold area of the resulting Hotellings T^2 statistics. The statistical maps are shown in Figure 3(a). The threshold for significance at each surface point was chosen to be p=0.05. Although sample sizes are small, we still detected large statistically significant areas, consistent with prior findings [8]. The permutation-based overall significance p values [16], corrected for multiple comparisons, were 0.0028, for the left ventricle and p=0.0066 for the right ventricle, respectively.

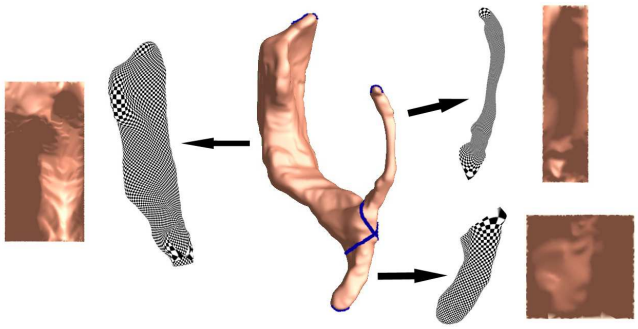

Fig. 2. Lateral ventricular surface registration via holomorphic one-forms. An example left ventricular surface is shown in the middle, with its segmentation results. After segmentation, a new canonical holomorphic one-form is computed on each piece and each piece is conformally mapped to a rectangle. Surface registration is performed via the parameter domain.

To explore whether our multivariate statistics provided extra power when running TBM on the surface data, we also conducted four additional statistical tests using different tensor-based statistics derived from the Jacobian matrix. The other statistics we studied were: (1) the pair of eigenvalues of the Jacobian matrix, treated as a 2-vector; (2) the determinant of Jacobian matrix; (3) the largest eigenvalue of Jacobian matrix; and (4) the smallest eigenvalue of Jacobian matrix. For statistics (1) we used Hotelling's T^2 statistics to compute the group mean difference. In cases of (2), (3) and (4), we applied a Students t test to compute the group mean difference at each surface point. For these four new statistics, their calculated statistical maps are shown in Figure 3(b)-(e), respectively.

	Full Matrix J	Determinant of J	Largest EV of J	Smallest EV of J	Pair of EV of J
Left Vent Surface	**0.0028**	0.0330	0.0098	0.0240	0.0084
Right Vent Surface	**0.0066**	0.0448	0.0120	0.0306	0.0226

Table 1. Permutation-based overall significance levels, i.e. corrected p values, are shown, after analyzing various different surface-based statistics (J is the Jacobian matrix and EV stands for Eigenvalue). To detect group differences, it was advantageous to use the full tensor, or its two eigenvalues together; with simpler local measures based on surface area, group differences were less powerfully detected.

For each statistic, we also computed the overall p-values (see Table 1). Areas of surface abnormalities detected by different tensor-based surface statistics were highly consistent. The experiments also strongly suggested that the newly proposed multivariate TBM method has more detection power in terms of effect size (and the area with suprathreshold statistics), probably because it captures more directional and rotational information when measuring geometric differences.

5. CONCLUSION AND FUTURE WORK

In this paper, we presented a multivariate tensor-based morphometry framework for analyzing parametric surfaces. The empirical experimental results demonstrated our method outperformed TBM methods based on simpler univariate surface measures. In future, we will apply this multivariate TBM framework to additional 3D MRI datasets to study brain surface morphometry. We plan to apply other holomorphic differentials to study related surface regularization, parameterization and registration problems.

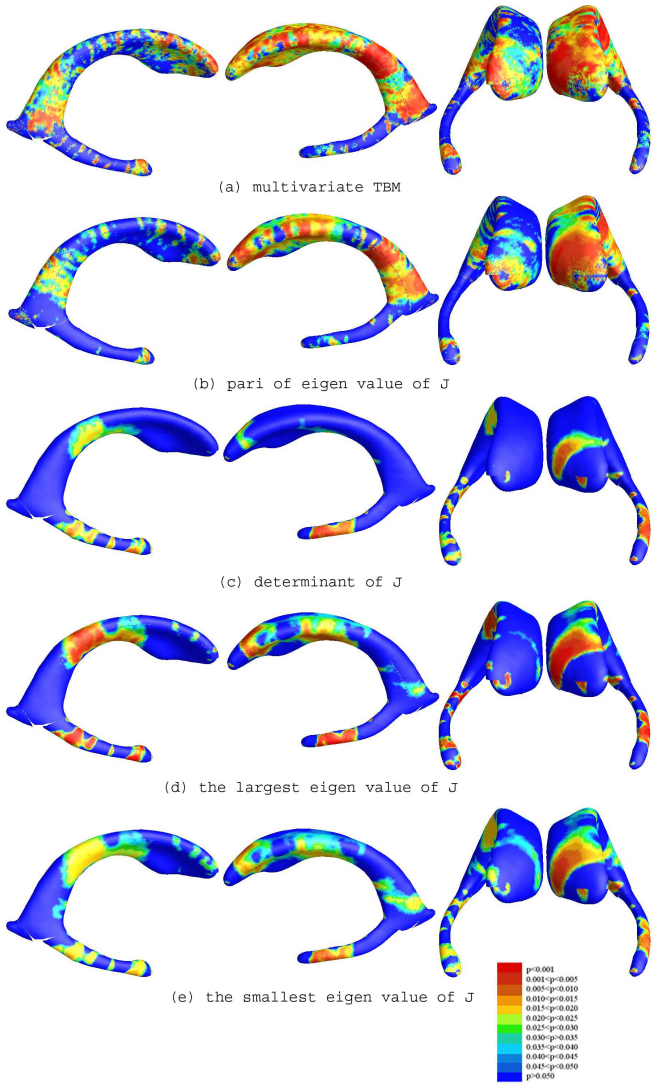

Fig. 3. Comparison of various tensor-based morphometry results on a group of lateral ventricular surfaces from 11 HIV/AIDS patients and 8 matched control subjects.

6. REFERENCES

[1] J. Ashburner, et al. *Hum Brain Mapp*, vol. 6, no. 5-6, pp. 348–357, 1998.

[2] M. K. Chung, et al. *Neuroimage*, vol. 14, pp. 595–606, 2001.

[3] L. Wang, et al. *NeuroImage*, vol. 20, no. 2, pp. 667 – 682, 2003.

[4] M. K. Chung, et al. *NeuroImage*, vol. 18, no. 2, pp. 198 – 213, 2003.

[5] C. Davatzikos, et al. *J Comput Assist Tomogr*, vol. 20, no. 1, pp. 88–97, 1996.

[6] P. M. Thompson, et al. *Nature*, vol. 404, no. 6774, pp. 190–193, March 2000.

[7] M.K. Chung, et al. *IEEE TMI*, vol. 27, no. 8, pp. 1143–1151, Aug. 2008.

[8] P. M. Thompson, et al. *NeuroImage*, vol 31, no. 1, pp. 12-23, 2006.

[9] O.T. Carmichael, et al. *Biomedical Imaging: Nano to Macro, 2006. 3rd IEEE International Symposium on*, pp. 315–318, April 2006.

[10] Luca Ferrarini, et al. *NeuroImage*, vol. 32, no. 3, pp. 1060 – 1069, 2006.

[11] Y. Chou, et al. *NeuroImage*, vol. 40, no. 2, pp. 615 – 630, 2008.

[12] Y. Wang, et al. *IEEE TMI*, vol. 26, no. 6, pp. 853–865, June 2007.

[13] N. Leporé, et al. *IEEE TMI*, vol. 27, no. 1, pp. 129–141, Jan. 2008.

[14] V. Arsigny, et al. in *Magn. Reson. Med.*, 2006, vol. 56, pp. 411–421.

[15] Y. Wang, et al. *2nd MICCAI Workshop on Mathematical Foundations of Computational Anatomy*, pp. 36–47, 2008.

[16] P. M. Thompson, et al. *J. Neurosciende*, pp. 4146–4158, 2005.